STUDIA UBB CHEMIA, LXV, 1, 2020 (p. 27-38)
(RECOMMENDED CITATION)
DOI:10.24193/subbchem.2020.1.03

PARACETAMOL DETECTION AT A GRAPHITE PASTE MODIFIED ELECTRODE BASED ON PLATINUM NANOPARTICLES IMMOBILISED ON Al-SBA-15 COMPOSITE MATERIAL

THI THANH HIEN NGO[a], IOANA CARMEN FORT[b], THANH HUYEN PHAM[a,*], GRAZIELLA LIANA TURDEAN[b,*]

ABSTRACT. A composite material was obtained by immobilizing platinum nanoparticles (Pt-NPs) within an ordered mesoporous structure Al-SBA15 (having improved acidity due to the presence of Al). This was used for preparing a graphite paste modified electrode (Pt/Al-SBA-15-GPE), which was applied for paracetamol (PA) detection. The obtained electrode was investigated by electrochemical methods (*e.g.* cyclic voltammetry, CV and electrochemical impedance spectroscopy, EIS), in order to estimate the electrochemical parameters, which were compared with those of GPE unmodified electrode. Square-wave voltammetry (SWV) was used to obtain the analytical parameters of Pt/Al-SBA-15-GPE for PA detection. The good analytical parameters recommend the composite mesoporous material (Pt/Al-SBA-15) to be used for preparing modified electrodes for PA detection in real samples.

Keywords: *Pt nanoparticles, ordered mesoporous structure, graphite paste modified electrode, paracetamol*

INTRODUCTION

Paracetamol (N-acetyl-para-aminophenol, abbreviated PA) is a substance used for medical treatment of pain and fever because of its analgesic and antipyretic properties. The determination of PA in pharmaceutical formulation use optical [1], chromatographic, capillary electrophoretic and electroanalytical

[a] *HaNoi University of Science and Technology, School of Chemical Engineering, 1 Dai Co Viet, Hanoi, Vietnam*
[b] *"Babes Bolyai" University, Faculty of Chemistry and Chemical Engineering, Department of Chemical Engineering, Center of Electrochemistry and Non-Conventional Materials, 11, Arany Janos, 400198 -Cluj-Napoca, Romania*
* *Corresponding authors: gturdean@chem.ubbcluj.ro and huyen.phamthanh@hust.edu.vn*

methods [2]. Electroanalytical methods based on chemically modified electrode have more advantages over the other conventional standardized methods due to relatively low cost, high sensitivity, fast response, miniaturization/portability and instrumental simplicity. Thus, the PA detection was realized using different chemically modified electrodes, containing conducting polymers [3-6], carbon nanotubes [3, 7-8], graphenes [9] and noble metal nanoparticles (NPs) [10].

SBA-15 (Santa Barbara Amorphous No. 15), developed in 1998 by Zhao et al. [11], is a relatively new mesoporous material intensively studied because of its inert and non-toxic hexagonal structure, which possesses a high degree of structural ordering, larger pore size, thicker pore walls, ease of synthesis, and higher hydrothermal/thermal stability. The application of this material in catalysis is hindered because of its poor acidity, consequently the incorporation of Al in the framework of SBA-15 has been reported (Al-SBA-15) [12]. Also, the strategy to prepare a composite material by immobilizing metal NPs (here Pt-NPs) within the porous structure of Al-SBA-15, could be adopted in order to exploit both the advantages offered by NPs, as well as of the high surface area and ordered structure from the mesoporous silica [13-14].

From the best of our knowledge is the first time when a Pt immobilized on a mesoporous compound SBA-15 (Pt/Al-SBA-15) was used as electrode material for PA detection. In this context, a modified electrode (Pt/Al-SBA-15-GPE) was prepared by including the composite material into a graphite paste matrix. The electrochemical parameters were obtained by investigating the modified electrode by cyclic voltammetry (CV) and electrochemical impedance spectroscopy (EIS). In order to estimate the analytic parameters, either *in vitro* or in real samples, square wave voltammetry (SWV) investigation method was used.

RESULTS AND DISCUSSION

Electrochemical behavior of Pt/Al-SBA-15-GPE electrode material

In Fig. 1 are presented the cyclic voltammograms in the presence of PA at Pt/Al-SBA-15-GPE and at unmodified GPE electrode (Fig. 1 inset), recorded with a scan rate of 50 mV s^{-1}. The peak pairs (A1/C1) placed at E_{pa} = +0.425 V *vs.* Ag|AgCl,KCl_{sat} and at E_{pc} = +0.312 V *vs.* Ag|AgCl,KCl_{sat} potentials, respectively are attributed to the PA redox behavior. An analogous behavior was recorded at MCPE-PtMWCNTs–TX100 modified electrode (*i.e.:* E_{pa} = 0.362 V and E_{pc} = 0.311 V [15], where MCPE = modified carbon paste electrode, MWCNTs = multi-walled carbon nanotubes). The estimated electrochemical parameters values were: peak-to-peak separations (computed $\Delta E = E_{pa} - E_{pc}$) of +0.113 V

at Pt/Al-SBA-15-GPE and +0.238 V at GPE and the formal potentials (computed $E^{0'} = (E_{pa} + E_{pc})/2$) of +0.369 V at Pt/Al-SBA-15-GPE and +0.377 V at GPE, respectively. Also, the anodic to cathodic peak currents ratio (computed I_{pa}/I_{pc}) were 1.99 at Pt/Al-SBA-15-GPE and 3.55 at GPE, respectively, proving that the oxidation process of PA is predominant, comparing with the reduction one. The decrease of the I_{pa}/I_{pc} ratio value in the presence of Pt-NPs in the sensing matrix (Pt/Al-SBA-15-GPE) indicates the diminution of the irreversible character of the studied electron transfer reaction encountered at the unmodified electrode (GPE).

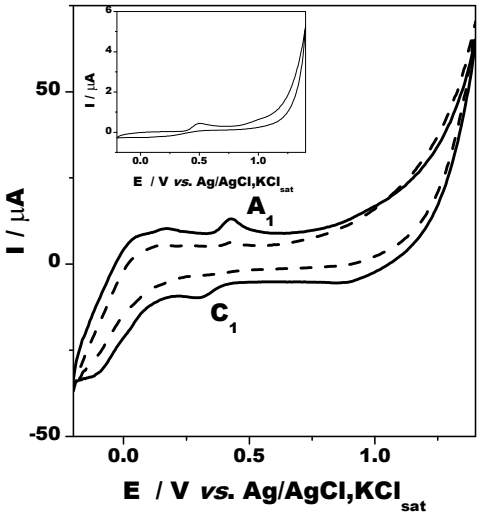

Figure 1. Cyclic voltammograms recorded at Pt/Al-SBA-15-GPE in absence (dot line) and in presence of 7 10^{-6} M PA (solid line). Inset: CV at unmodified GPE in presence of 7 10^{-6} M PA. Experimental conditions: electrolyte, 0.1 M phosphate buffer (pH 7); scan rate, 50 mV s^{-1}; starting potential, -0.2 V *vs.* Ag/AgCl, KCl_{sat}.

The full width at half of the peak maximum height (FWHM) is 107 mV and 83 mV for Pt/Al-SBA-15-GPE modified electrode and GPE unmodified electrode, respectively. Generally, values of FWHM that are different than the theoretical one (*i.e.,* 90.6/n [mV]) have been attributed to electrostatic effects due to the presence of adjacent charged species [16].

The calculation of the number of electrons involved in the PA electrooxidation process is based on Eq. 1 [17, 18, 19]:

$$E_{p,a} - E_{p,a/2} = 47.7/ \alpha n_a \text{ (mV at 25 °C)} \quad (1)$$

where: $E_{p,a/2}$ is the half-peak oxidation potential, α is the electron transfer coefficient, n_a is the number of transferred electrons in the oxidation reaction.

At 0.05 V s^{-1}, the $E_p - E_{p/2}$ values are +37 mV and -52 mV for anodic and cathodic peak (A1/C1), respectively. Consequently, for an electron transfer coefficient (α) assumed as 0.5, the number of transferred electrons is 2. The obtained value is in accordance with the mechanism presented in literature, where PA is involved into a redox reaction transferring two electrons and two protons to form N-acetyl-p-quinone imine [15, 20, 21] (Scheme 1):

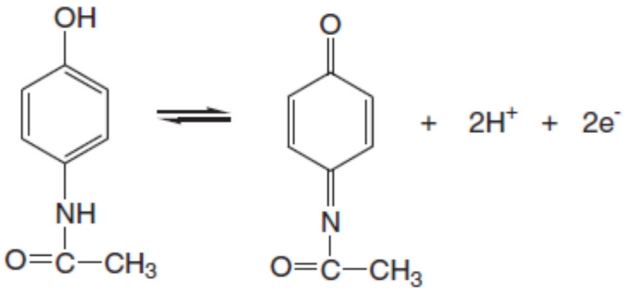

PA N-acetyl-p-quinone imine

Scheme 1

As expected, the influence of the increase of potential scan rate on the voltammograms shape, recorded in the presence of PA at Pt/Al-SBA-15-GPE (Fig. 2), shows a shift towards positive and negative direction of the anodic and cathodic potential peak (A1/C1), respectively. The values of the slopes of the log I - log v dependencies (Fig. 2 inset) for the oxidation/reduction peaks presented in Table 1 are close to the theoretical value from equation 2 (*i.e.,* 0.5).

$$I_p = (2.99\ 10^5)\ n(\alpha n)^{1/2}\ A\ C_o\ D^{1/2}\ v^{1/2} \quad (2)$$

where: n is the number of electrons, α is the electron transfer coefficient, A is the active surface area (cm^2), C_o is the concentration in bulk solution (mol/cm^3), D is the diffusion coefficient (cm^2/s) and v is the scan rate (V/s) [18, 19].

This behavior indicates a diffusion-controlled redox process of PA oxidation occurring to the Pt/Al-SBA-15-GPE modified electrode [18, 19, 22].

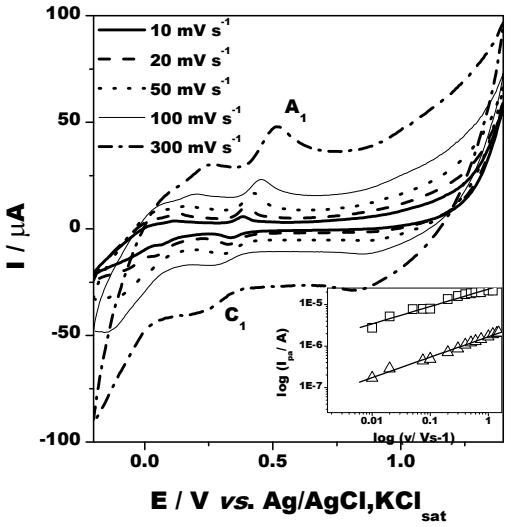

Figure 2. Cyclic voltammograms recorded at Pt/Al-SBA-15-GPE in the presence of 7 10^{-6} M PA at different scan rate. Inset: the influence of scan rate on anodic peak currents intensities at Pt/Al-SBA-15-GPE (□) and GPE (∆) electrodes. Experimental conditions: electrolyte, 0.1 M phosphate buffer (pH 7); starting potential, -0.2 V *vs*. Ag/AgCl, KCl_{sat}.

Table 1. Slope of log I *versus* log v dependency. Experimental conditions: see Fig 2.

Electrode type	Slope R / n	
	anodic	cathodic
GPE	0.491 ± 0.011 / 0.9969 / 14	0. 405 ± 0.015 / 0.9919 / 14
Pt/Al-SBA-15-GPE	0.418 ± 0.024 / 0.9823 / 13	-

Stability of Pt/Al-SBA-15-GPE modified electrode

The short-time stability was tested by continuous cycling (20 cycles) the Pt/Al-SBA-15-GPE modified electrode potential, immersed in phosphate buffer (pH 7), with a scan rate of 50 mV s^{-1}. The mean value of the absolute current intensities was 31.5 ± 0.02 µA (RSD 1.98 %, for anodic process) and of 19.5 ± 0.01 µA (RSD 0.52%, cathodic process) respectively.

The long-term stability was tested by recording cyclic voltammograms in the presence of 7 10^{-6} M PA, at the Pt/Al-SBA-15-GPE modified electrode with a scan rate of 50 mV s^{-1}, in several days after their preparation. The results revealed that after 7 days of storage in water saturated atmosphere (at 4 °C), the oxidation/reduction current intensities of PA have had a relative decrease from their original responses with 41.5% and 16.6%, respectively (estimated as: $(I_{day1} - I_{day7})*100/I_{day7}$). This behaviour demonstrates that the Pt/Al-SBA-15-GPE modified electrode possessed an acceptable reusability capacity [23].

Electrochemical impedance spectroscopy measurements at Pt/Al-SBA-15-GPE electrode

The Nyquist plots recorded in a redox probe of 1 mM $K_3[Fe(CN)]_6/K_4[Fe(CN)]_6$ at Pt/Al-SBA-15-GPE and GPE electrodes, respectively, are shown in Fig. 3. The depressed semicircle observed at Pt/Al-SBA-15-GPE interface is characteristic to porous materials [24], indicating low interfacial electron transfer resistance and good conductivity. Contrarily, at GCE electrode a remarkable capacitive loop is present.

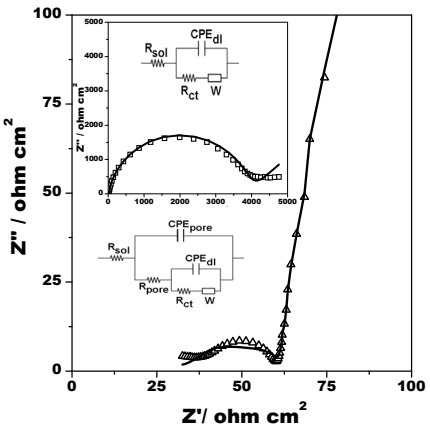

Figure 3. Nyquist plots recorded at Pt/Al-SBA-15-GPE modified electrode (△) and GPE unmodified electrode (□) (inset) into a solution containing 1 mM $K_4[Fe(CN)_6]/K_3[Fe(CN)_6]$ + 0.1 M phosphate buffer (pH 7). Experimental conditions: frequency, 10^{-2} – 10^4 Hz; amplitude, 10 mV; time for OCP, 60 s; experimental data (symbol), fitted data (solid line).

Both equivalent electric circuit used for fitting the obtained experimental data (see inset Fig. 3, Table 2) consists from parallel and serially connected resistors (R_{sol}, R_{ct} R_{pore}), constant phase elements (CPE_{dl}, CPE_{pore}) and Warburg impedance element (W), respectively. The R_{sol} represents the resistance of the electrolyte at the interface of the mesoporous material, R_{ct} is the charge transfer resistance, and R_{pore} is the intrinsic material resistance [25]. The CPE_{dl} is the constant phase element corresponding to the double layer capacitance, CPE_{pore} is the constant phase element corresponding to the pore capacitance, and W is an element representing the restricted diffusion of ions through the multiple layers of non-homogenous distributed pores through the internal mesoporous network of the material.

As expected, at GPE the great R_{ct} value indicates a hindering of the electron transfer process, while in the case of Pt/Al-SBA-15-GPE modified electrode a 10 times decrease of the R_{ct} (Table 2) point out an easy electron transfer occurring at electrode interface, probably due to the presence of Pt-NPs on the mesoporous structure of the Al-SBA-15 material.

Table 2. EIS fitting parameters for Pt/Al-SBA-15-GPE modified electrodes. Experimental conditions: see Fig 3.

EIS parameters	GPE *	Pt/Al-SBA-15-GPE **
R_{sol} (Ω cm^2)	13.36 ± 1.24	31.24 ± 2.77
CPE_{pore} (S s^n/cm^2)	-	142.6 10^{-5} ± 2.41
n_1	-	0.496
R_{pore} (Ω cm^2)	-	33.12 ± 6.61
CPE_{dl}(S s^n/cm^2)	1.127 10^{-5} ± 1.71	7049.0 10^{-5} ± 10
n_2	0.905	1
R_{ct} (Ω cm^2)	3917 ± 0.76	273 ± 8
W (S $s^{1/2}$ / cm^2)	337.4 10^{-5} ± 6.98	529.6 ±10^{-5} + 3.4
chi^2	0.629 10^{-3}	0.964 10^{-3}

± values are relative standard errors expressed as %; * fitted by $R_{sol}(CPE_{dl}(R_{ct}W))$ electric circuit [26, 27]; ** fitted by $R_{sol}(CPE_{pore}(R_{pore}(CPE_{dl}(R_{ct}W))))$ electric circuit.

Analytical characterization of Pt/Al-SBA-15-GPE electrode material Calibration curve

The quantitative analysis of PA was carried out investigating the Pt/Al-SBA-15-GPE modified electrode by square wave voltammetry (Fig 4A). The calibration curve shows excellent linearity in a concentration range between 10^{-6} – 10^{-5} M PA. The linear regression equations are: I/A = (-8.36 10^{-7} ± 2.66 10^{-7}) + (1.68 ± 0.04) [PA]/M (R = 0.9968, n = 11 points) and I/A = (2.8 10^{-9} ± 3.07 10^{-9}) + (29.9 10^{-3} ± 0.5 10^{-3}) [PA]/M (R = 0.9986, n = 11 points) at Pt/Al-SBA-15-GPE modified electrode and GPE, respectively (Fig 4B). The increase of approximatively 60 times of the sensitivity of the Pt/Al-SBA-15-GPE modified electrode, compared with the unmodified GPE electrode, is due to the presence of Pt-NPs in the Pt/Al-SBA-15-GPE composite material of the electrode matrix.

The detection limit estimated for a signal-to-noise ratio (S/N) of 3 were of 0.85 10^{-6} M at Pt/Al-SBA-15-GPE modified electrode. The obtained values are lower comparatively with some reported in the literature 1.1 10^{-6} M at CPE-CNT-poly(3-aminophenol) [4], 2.3 10^{-6} M at C-Ni/GCE [28], 1.39 10^{-6} M at PEDOT/SPE [29], and 6 10^{-6} M at graphene oxide-GCE [30].

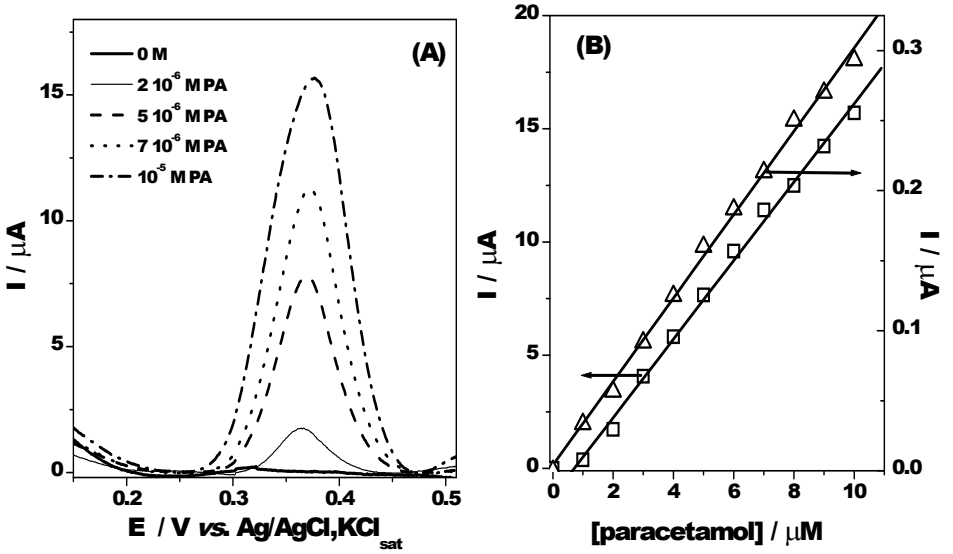

Figure 4. Square wave voltammograms recorded in the presence of different concentration of PA (see inset) at Pt/Al-SBA-15-GPE modified graphite paste electrode (**A**) and calibration curve of Pt/Al-SBA-15-GPE modified graphite paste electrode (∆) and GPE (□) for PA (**B**). Experimental conditions: electrolyte, 0.1 M phosphate buffer (pH 7); frequency, 25 Hz; amplitude, 10 mV; step potential, 0.75 mV; starting potential, -0.2 V *vs*. Ag/AgCl, KCl_{sat}.

Interferences

The possible interference for the determination of PA was also studied, under the same experimental conditions. Thus, the oxidation peak for a concentration of 7 10^{-6} M PA was individually measured in the presence of different concentrations of the most common interfering compounds, like: 0.9 mM ascorbic acid and 1 10^{-6} M uric acid. Their concentrations were chosen in the therapeutic concentration window. From Fig. 5, it can be seen that there is almost no influence on the detection of PA, because the peaks corresponding to the interfering compounds appear completely separated from the oxidation peak of PA.

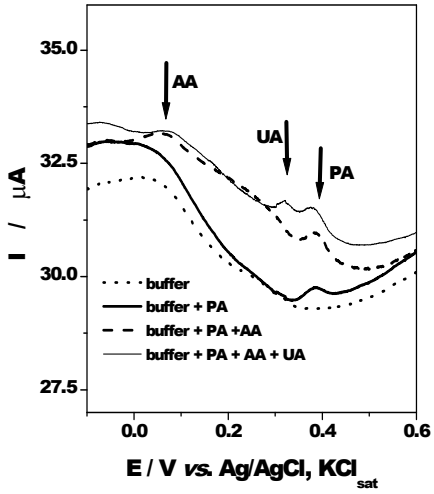

Figure 5. Square wave voltammograms recorded at Pt/Al-SBA-15-GPE modified electrode in the presence of a mixture of 7 10^{-6} M paracetamol, 0.9 10^{-3} M ascorbic acid and 1 10^{-6} M uric acid. Experimental conditions: electrolyte, 0.1 M phosphate buffer (pH 7); frequency, 25 Hz; amplitude, 10 mV; step potential, 0.75 mV; starting potential, -0.2 V *vs*. Ag/AgCl, KCl_{sat}.

Real sample analysis

The Pt/Al-SBA-15-GPE modified electrode was used to estimate the PA concentration in different commercial tablets, using the standard addition method, appropriate when the samples have complex matrices. The SWV measurements were performed using three different Pt/Al-SBA-15-GPE electrodes and the obtained data were used to calculate the average value of the PA concentration for the analyzed samples (Table 3). The results obtained in similar experimental conditions as for the electrode calibration against PA, were found in very good agreement with those declared by the pharmaceutical tablets producer (Table 3). It was found that the recovery of PA was in the range of 96.99 – 102.21 %. The relative standard deviation (RSD) was smaller than 3 %. The excellent average recoveries for the real samples suggest that the studied electrode material (Pt/Al-SBA-15-GPE) is able to be used for PA detection from pharmaceutical tablets.

Table 3. Determination of PA from pharmaceutical tablets using Pt/Al-SBA-15-GPE modified electrode.

Sample	**Added/** µM	**Found/** µM	**Recovery %**	**RSD %**
PA (500 mg/tablet)	5	4.95 ± 0.13	99.6 ± 2.61	2.63

* Mean values obtained using 3 different electrodes

CONCLUSIONS

A composite material (Pt/Al-SBA-15) based on the immobilization of Pt-NPs on a high ordered mesoporous compound (Al-SBA-15) was used to develop an electrode for electrochemical detection of paracetamol. The characterization consisted in using electrochemical methods of investigation like: cyclic voltammetry, electrochemical impedance spectroscopy and square-wave voltammetry.

The comparison of electrochemical parameters obtained in the case of Pt/Al-SBA-15-GPE modified electrode and GPE unmodified electrode suggest that the presence of Pt-NPs in the high ordered structure of the mesoporous material Al-SBA-15 enhanced the electrochemical and analytical parameters.

The very good analytical parameters (high sensibility, low limit of detection, good stability, no interference) recommend the studied compound Pt/Al-SBA-15, for the use as electrode material for paracetamol detection in real samples.

EXPERIMENTAL SECTION

Chemicals

As described previously, the 1% Pt/Al-SBA-15 material was prepared by a wet impregnation methodology [31]. Graphite powder and paraffin oil (Sigma-Aldrich) were used for preparing graphite paste electrode (GPE). A 0.1 M phosphate buffer solution was prepared from KH_2PO_4 and K_2HPO_4 (Merck, Darmstadt, Germany) salts. The pH of the buffer solutions was adjusted to the desired value by adding H_3PO_4 or KOH solutions (Merck, Darmstadt, Germany). A 1 mM $K_3[Fe(CN)]_6/K_4[Fe(CN)]_6$ solution was prepared by dissolving the appropriate weights of salts obtained from Sigma-Aldrich in phosphate buffer (pH 7). Synthetic paracetamol (PA) was purchased from Terapia-Rambaxy, (Cluj-Napoca, Romania) and used for preparing the standard solutions (1 mM). Distilled water was used for preparing all solutions. All reagents were of analytical degree and were used without further purification.

Drugs containing 500 mg PA/tablet (“Paracetamol” from EuroPharm SA) were bought from local pharmacies. Three tablets were weighed and grounded in a mortar. A quantity of the obtained homogeneous powder equivalent to the average weight of one tablet was dissolved in 0.1 M phosphate buffer solution (pH 7). After sonication for 10 min, the fresh prepared solution was analyzed, applying the standard addition method.

Preparation of Pt/Al-SBA-15-GPE modified electrode

The Pt/Al-SBA-15-GPE modified electrode was prepared by thoroughly mixing 20 mg of graphite powder and 20 mg Pt/Al-SBA-15 powder with 15 mL of paraffin oil. The obtained paste was put into the cavity of a Teflon holder. The obtained electrode surface was smoothed using paper. When necessary, a new electrode surface was obtained by removing 2 mm of the outer paste layer, and adding freshly modified paste.

Electrochemical measurements

All electrochemical measurements (cyclic voltammetry, electrochemical impedance spectroscopy and square wave voltammetry) were performed using a PC controlled electrochemical analyzer (AUTOLAB). A conventional three-electrodes cell equipped with a working electrode (Pt/Al-SBA-15-GPE modified electrode or GPE unmodified electrode, with a geometrical area of 0.07 cm^2), a counter electrode (Pt wire), and a reference electrode (Ag|AgCl,KCl_{sat}) was used. The experimental conditions are presented in the capture of each figure.

ACKNOWLEDGMENTS

Thi Thanh Hien NGO gratefully acknowledges the Erasmus+ Program with partner countries for the financial support of her stage at “Babes-Bolyai” University from Cluj-Napoca (Romania).

REFERENCES

1. X. Liu, W. Na, H. Liu, X. Su, *Biosens. Bioelectron.*, **2017**, *98*, 222-226.
2. M. Espinosa Bosch, A.J. Ruiz Sanchez, F. Sanchez Rojas, C. Bosch Ojeda, *J. Pharm. Biomed. Anal.*, **2006**, *42*, 291-321.
3. E. Bayram, E. Akyilmaz, *Sensor. Actuat. B*, **2016**, *233*, 409-418.
4. I. Noviandri, R. Rakhmana, *Int. J. Electrochem. Sci.*, **2012**, *7*, 4479-4487.
5. J. Luo, J. Sun, J. Huang, X. Liu, *Chem. Eng.*, **2016**, *283*, 1118-1126.
6. Y. Teng, L. Fan, Y. Dai, M. Zhong, X. Lu, X. Kan, *Biosens. Bioelectron.*, **2015**, *71*, 137-142.
7. P. K. Kalambate, A. K. Srivastava, *Sensor. Actuat. B*, **2016**, *233*, 237-248.
8. A. Kutluay, M. Aslanoglu, *Sensor. Actuat. B*, **2013**, *185*, 398-404.
9. X. Kang, J. Wang, H. Wu, J. Liu, I. A. Aksay, Y. Lin, *Talanta*, **2010**, *81*, 754-759.
10. P. K. Kalambate, B. J. Sanghavi, S. P. Karna, A. K. Srivastava, *Sensor. Actuat. B*, **2015**, *213*, 285-294.

11. D. Zhao, J. Feng, Q. Huo, N. Melosh, G. H. Fredrickson, B. F. Chmelka, G. D. Stucky, *Science*, **1998**, *279*, 548-552.
12. Y. Yue, A. Gédéon, J.-L. Bonardet, N. Melosh, J.-B. D'Espinose, J. Fraissard, *Chem. Commun.*, **1999**, *19*, 1967-1968.
13. H.-C. Wu, T.-C. Chen, N.-C. Lai, C.-M. Yang, J.-H. Wu, Y.-C. Chen, J.-F. Lee, C.-S. Chen, *Nanoscale*, **2015**, *7*, 16848-16859.
14. S. Hazra, H. Joshi, B. K. Ghosh, A. Ahmed, T. Gibson, P. Millner, N. N. Ghosh, *RSC Adv.*, **2015**, *5*, 34390-34397.
15. O. J. D'Souza, R. J. Mascarenhas, T. Thomas, B. M. Basavaraja, A. Kumar Saxena, K. Mukhopadhyay, D. Roy, *J. Electroanal. Chem.*, **2015**, *739*, 49-57.
16. A. L. Eckermann, D. J. Feld, J. A. Shaw, T. J. Meade, *Coord. Chem. Rev.*, **2010**, *254*, 1769–1802.
17. P. K. Kalambate, A. K. Srivastava, *Sensor. Actuat. B*, **2016**, *233*, 237–248.
18. A. J. Bard, L. R. Faulkner, "Electrochemical Methods: Fundamentals and Applications", VCH-Wiley, **2011**.
19. C. M. A. Brett, A. M. O. Brett, "Electrochemistry. Principles, methods, and applications", Oxford University Press, New York, NY, USA, **1994**.
20. B. J. Sanghavi, A. K. Srivastava, *Electrochim. Acta*, **2010**, *55*, 8638-8648.
21. M. Zheng, F. Gao, Q. Wang, X. Cai, S. Jiang, L. Huang, F. Gao, *Mater. Sci. Eng. C*, **2013**, *33*, 1514-1520.
22. S. Kavian, S. N. Azizi, S. Ghasemi, *J. Electroanal. Chem.*, **2017**, *799*, 308-314.
23. R. Gupta, V. Ganesan, *Sensor. Actuat. B*, **2015**, *219*, 139-145.
24. F. J. Burpo, E. A. Nagelli, L. A. Morris, J. P. McClure, M. Y. Ryu, J. L. Palmer, *J. Mater. Res.*, **2017**, *32*, 4153-4165.
25. I. C. Fort, G. L. Turdean, R. Barabas, D. Popa, A. Ispas, M. Constantiniuc, *Studia UBB Chemia*, **2019**, *64*, 125-133.
26. G.L. Turdean, C.I. Fort, V. Simon, *Electrochim Acta* **2015**, *182*, 707-714.
27. M. M. Rusu, C. I. Fort, L. C. Cotet, A. Vulpoi, M. Todea, G. L. Turdean, V. Danciu, I. C. Popescu, L. Baia, *Sensor. Actuat. B*, **2018**, *268*, 398-410.
28. S. Wang, F. Xie, R. Hu, *Sensor. Actuat. B*, **2007**, *123*, 495-500.
29. W. Su, S. Cheng, *Electroanal.*, **2010**, *22*, 707-714.
30. J. Song, J. Yang, J. Zeng, J. Tan, L. Zhang, *Sensor Actuat. B*, **2011**, *155*, 220–225.
31. C. Rizescu, B. Cojocaru, N. T. Thanh Hien, P. T. Huyen, V. I. Parvulescu, *Micropor. Mesopor. Mat.*, **2019**, *281*, 142-147.